

Medium effect on the nuclear modification factor of protons and pions in intermediate-energy heavy ion collisions

M. Lv (吕明),^{1,2} Y. G. Ma (马余刚),^{1,3,*} J. H. Chen (陈金辉),¹ D. Q. Fang (方德清),¹ and G. Q. Zhang (张国强)¹

¹Shanghai Institute of Applied Physics, Chinese Academy of Sciences, Shanghai 201800, China

²University of Chinese Academy of Sciences, Beijing 100049, China

³ShanghaiTech University, Shanghai 200031, China

(Received 10 September 2015; revised manuscript received 1 January 2017; published 21 February 2017)

Nuclear modification factors R_{cp} of protons and pions are investigated by simulating Au+Au collisions from 0.8A to 1.8A GeV in a framework of an isospin-dependent quantum molecular dynamics (IQMD) model. The R_{cp} of protons rise with an increase in the transverse particle momentum p_T at different beam energies owing to radial flow and the multiple-collision effect. The rate of increase of R_{cp} is suppressed at higher beam energies. While the R_{cp} of pions display weaker p_T dependence. By changing the in-medium nucleon-nucleon cross section, the R_{cp} of protons change a lot, while the R_{cp} of pions do not. In addition, by deactivating the $N\Delta \rightarrow NN$ and $\pi N \rightarrow \Delta$ channels, the R_{cp} of protons change slightly in their increasing rates compared with the “original” case (with these two channels). However, the R_{cp} of pions is shifted down for the “no $N\Delta \rightarrow NN$ ” case and has an inverse trend for the “no $\pi N \rightarrow \Delta$ ” case. Based on these observations, we argue that the observable R_{cp} is a suitable tool to better distinguish in-medium effects of protons and pions.

DOI: [10.1103/PhysRevC.95.024614](https://doi.org/10.1103/PhysRevC.95.024614)

I. INTRODUCTION

One of the main goals of research in intermediate-energy heavy ion collisions (HICs) has focused on learning the bulk properties of hot and compressed nuclear matter and its transport mechanisms over the last 30 years [1–3]. Transport models such as the Boltzmann-Uehling-Uhlenback (BUU) type [4,5] and quantum molecular dynamics (QMD) type [1,3] have been successful in describing the reaction dynamics of intermediate-energy heavy ion collisions. The two main ingredients of the nuclear transport process are the nucleonic mean field and nucleon-nucleon (NN) binary interaction. Recently, the medium effects on nucleon-nucleon cross sections (NNCSs) have been widely investigated by replacing the NNCS in vacuum with an in-medium one [6–11]. Since a high-density region for compressed nuclear matter could be reached up to 2–3 times the normal nuclear matter density ρ_0 before it expands during the process of heavy ion collisions at 1A–2A GeV, the in-medium NNCS is therefore an important component in these phenomenological simulations due to its close relation with the density.

The nuclear modification factor (NMF) has been extensively studied in relativistic heavy ion collisions in recent years [12–18]. In these studies, unanimous results have demonstrated that the NMF is suppressed at high p_T owing to the strong partonic energy loss effect. However, the R_{cp} of protons show a rise with p_T at the low and moderate p_T range in intermediate energy HICs, which was argued to be an indication of a combined effect from radial flow and Cronin effect [19]. A scaling behavior of nuclear modification factor of pions and protons has been also investigated based on the available data of the transverse momentum spectra in relativistic energies and a number of constituent quark

(NCQ) scaling behavior of pions and protons for NMF was exhibited [20]. Meanwhile, a number of constituent nucleon scaling behavior of light nuclei for NMF was also found [20]. On the other hand, the nuclear stopping can provide the information on the nuclear equation of state (EoS), in medium nucleon-nucleon cross section as well as the degree of equilibrium [21,22]. Furthermore, the magnitude of nuclear stopping may have a direct relationship with the enhancement of R_{cp} . Besides, some other physical quantities, such as radial flow, temperature and viscosity, can also provide abundant information about dense hadronic matter formed in heavy ion collisions [23–27].

In the present work, the nuclear modification factors R_{cp} of protons and pions at different incident energies are investigated systematically. The nuclear medium effect from in-medium NNCSs are studied, while the pion absorption effect is also discussed.

The article is organized as follows. In Sec. II a brief introduction to the isospin-dependent QMD (IQMD) model is given. Section III describes pion dynamics in the IQMD model from which the pion spectra are compared with the FOPI experimental results and a preferable matching is obtained. The R_{cp} of p and π versus p_T and the radial flow are calculated at different incident energies in Sec. IV. Then we turn to the study of in-medium nucleon-nucleon cross sections which indicates the effective nucleon-nucleon interaction in the dense matter environment in Sec. V. At last, the effects of pion absorption and scattering processes are investigated in Sec. VI. A summary is given in the last section.

II. BRIEF DESCRIPTION OF IQMD MODEL

The quantum molecular dynamics model is a transport model based on a many-body theory to describe heavy ion collisions from intermediate to relativistic energies [1,3,28,29]. An extended version, the so-called the isospin-dependent

*Corresponding author: yigma@sinap.ac.cn

QMD model (IQMD) considers the isospin effects, which are suitable to investigate asymmetric nuclear systems. The QMD-type model can successfully treat collective flow, multifragmentation, isospin effects, transport coefficients, giant resonance, strangeness production, etc. [25,30–37].

In this framework, each nucleon is represented by a Gaussian wave packet in coordinate and momentum space to partially take into account the quantum effects,

$$\phi_i(\vec{r}, t) = \frac{1}{(2\pi L)^{3/4}} \exp\left(-\frac{[\vec{r} - \vec{r}_i(t)]^2}{4L}\right) \exp\left(\frac{i\vec{r} \cdot \vec{p}_i(t)}{\hbar}\right), \quad (1)$$

where \vec{r}_i and \vec{p}_i are the time-dependent variables that describe the center of the packet in coordinate and momentum space, respectively. The parameter L , related to the width of the wave packet in coordinate space, is determined by the size of the reaction system. Usually $L = 2.16 \text{ fm}^2$ for a Au+Au system.

The equation of motion for the center of the wave packet evolves according to the classical equation of motion based on the Hamiltonian of the system from effective nucleon interactions. The effective mean field used in the IQMD model can be expressed as

$$U = U_{\text{Sky}} + U_{\text{Coul}} + U_{\text{Yuk}} + U_{\text{sym}}, \quad (2)$$

where U_{Sky} , U_{Coul} , U_{Yuk} , and U_{sym} are the bulk Skyrme potential, the Coulomb potential, the surface Yukawa potential, and the isospin asymmetry potential, respectively. The bulk Skyrme potential is

$$U_{\text{Sky}} = \alpha \left(\frac{\rho}{\rho_0}\right) + \beta \left(\frac{\rho}{\rho_0}\right)^\gamma + \frac{\rho}{\rho_0} \int d\vec{p}' g(\vec{p}') \delta \ln^2[\epsilon(\vec{p} - \vec{p}')^2 + 1], \quad (3)$$

where ρ_0 is the saturation density at ground state, $g(\vec{p}, t) = \frac{1}{(\pi\hbar)^{3/2}} \sum_i e^{-[\vec{p} - \vec{p}_i(t)]^2 \frac{2L}{\omega^2}}$ is the momentum distribution function, $\rho = \sum_{ij} \rho_{ij}$ is the interaction density, and α , β , and γ are the Skyrme parameters, which connect tightly with the equation of state (EOS) of the bulk nuclear matter.

In this work, we use the soft EOS with momentum-dependent interaction. The corresponding parameters are $\alpha = -319 \text{ MeV}$, $\beta = 320 \text{ MeV}$, $\gamma = 1.14$, $\delta = 1.57 \text{ MeV}$, and $\epsilon = 500 \frac{c^2}{(\text{GeV})^2}$.

The expressions of the other potentials can be found in Ref. [1]. Within the present framework, reasonable phase-space information on nucleons and fragments in intermediate-energy heavy ion collisions can be obtained.

III. Δ PRODUCTION, Δ DECAY, AND π DYNAMICS

In the present work, the production of π is considered when inelastic scattering occurs. Pions are produced via the decay of a Δ resonance. The following inelastic reaction channels have been taken into account explicitly at the 1A GeV domain [38]:

- (a) $NN \rightarrow N\Delta$ (hard Δ production),
- (b) $\Delta \rightarrow N\pi$ (Δ decay),
- (c) $\Delta N \rightarrow NN$ (Δ absorption),
- (d) $N\pi \rightarrow \Delta$ (soft Δ production). (4)

In processes (a) and (d), the experimental cross section and the elastic NN collision are used [39]. In the energy domain of this work, elastic NN , $N-\Delta$, $\Delta-\Delta$, and πN scattering channels are taken into account; the $\pi-\pi$ scattering channel is not. Also, the higher mass resonance N^* is not considered because its contribution is negligible in this energy domain. Elastic and inelastic nucleon-nucleon scattering can be parametrized by the work of Huber and Aichelin, the details can be found in Ref. [39]. Of course, more complete channels on pion production could be considered in the near future in a QMD model as they were implemented in the coupled-channel-BUU model by Tesi *et al.* [40].

Pions produced via Δ decay propagate with a high thermal velocity under the Coulomb force. The different isospin channels have been considered and the branch ratios use the Clebsch-Gordan coefficient:

- (a) $\Delta^{++} \rightarrow 1(p + \pi^+)$,
- (b) $\Delta^+ \rightarrow 2/3(p + \pi^0) + 1/3(n + \pi^+)$,
- (c) $\Delta^0 \rightarrow 2/3(n + \pi^0) + 1/3(p + \pi^-)$,
- (d) $\Delta^- \rightarrow 1(n + \pi^-)$. (5)

After a π is produced, it has two evolutionary processes, namely, the π absorption process ($\pi NN \rightarrow \Delta N \rightarrow NN$) and π scattering process ($\pi N \rightarrow \Delta \rightarrow \pi N$).

In our previous publication, the p_T spectra of light charged particles (p , d , t) were shown to reproduce the experimental data very well [19]. In this work, the π spectra from the IQMD model with a soft equation of state with a momentum-dependent interaction (SM-EOS) are compared with the FOPI result: It shows that the yields of charged and neutral π measured around midrapidity (± 0.2) in Au+Au collisions at 1A GeV by IQMD simulation are comparable with the FOPI results [41]. Under the ‘‘minimum-bias’’ condition, pions are chosen in the rapidity range $-0.2 < Y/Y_{\text{proj}} < 0.2$, where Y_{proj} is the rapidity of the projectile nucleus. Figure 1 shows that

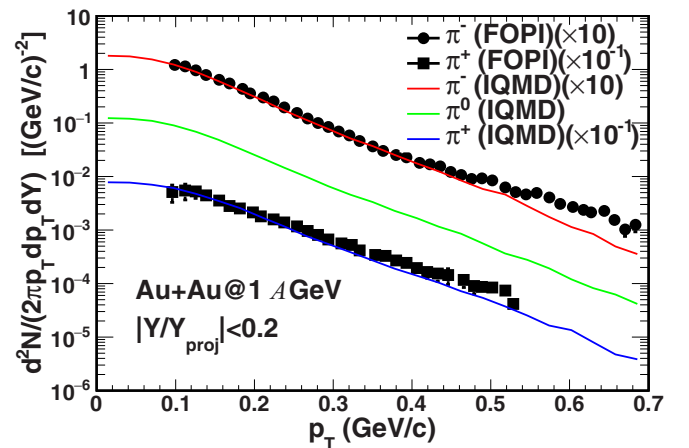


FIG. 1. Comparison of the π production cross section of the measurement and our simulations for midrapidity pions in Au+Au collisions at 1A GeV. The circle represents the FOPI data of π^- and the square for π^+ , the red, green, and blue lines represent different types of π from our IQMD simulations. In the calculations, $\pi N \rightarrow \Delta$ and $N\Delta \rightarrow NN$ are taken into account and the in-medium correction for NNCS is not used [i.e., $\eta = 0$ in Eq. (8)].

the spectra can match well with experimental data except for a little underestimation in higher p_T regions because all pions are only produced by Δ decay in our QMD model calculations.

IV. NUCLEAR MODIFICATION FACTOR R_{cp}

To study the nuclear medium effect in nucleus-nucleus collisions, it is convenient to introduce a ratio R_{cp} of the particle yield in central collisions to that in peripheral collisions [12,42]. R_{cp} is defined as follows:

$$R_{cp} = \frac{\left(\frac{d^2N}{2\pi p_T dp_T dY}\right)^C / N_{coll}^C}{\left(\frac{d^2N}{2\pi p_T dp_T dY}\right)^P / N_{coll}^P}, \quad (6)$$

where $\frac{d^2N}{2\pi p_T dp_T dY}$ is the particle invariant differential yield of the transverse momentum spectra p_T , N_{coll} means the nucleon-nucleon binary collision number, and the characters C and P stand for the central collision and peripheral collision, respectively. Both yield spectra are normalized by $\langle N_{coll} \rangle$ (binary scaling). If a nucleus-nucleus collision is a mere superposition of independent N_{coll} nucleon-nucleon collisions, the R_{cp} would be unity. Thus any departures from $R_{cp} = 1$ indicate the nuclear medium effects.

In the present work, Au+Au collisions at 0.8A, 1.0A, 1.2A, 1.5A, and 1.8A GeV are simulated with the IQMD model for the soft EOS with momentum-dependent interaction (SM+MDI). The double-differential transverse momentum spectra $\frac{d^2N}{2\pi p_T dp_T dY}$ of protons (pions) at different centralities (0–20%, 20–40%, 40–80%) have been obtained with the c.m.s. rapidity cut ($|Y/Y_{proj}| < 0.1$, where Y_{proj} is the initial projectile rapidity). All the R_{cp} in this work are obtained by dividing the spectra in the centrality of 0–20% to the one in the centrality of 40–80%.

A. R_{cp} of p and π at different energies

Figure 2 shows the R_{cp} of p and π at beam energies 0.8A–1.8A GeV. It is seen that the R_{cp} of p enhances quickly as p_T increases at different beam energies in Fig. 2(a), while the R_{cp} of π increases at low p_T and levels off at high p_T as shown in Fig. 2(b). For protons, the strength of R_{cp} enhancement is suppressed at high p_T with the increase in beam energy. We noticed that this energy dependence of R_{cp} is quite similar to the preliminary results of R_{cp} obtained at the BNL Relativistic Heavy Ion Collider (RHIC) [43] which show a monotonic evolution with collision energy from the enhancement versus p_T at low collision energy due to the Cronin effect and/or radial flow effect to the suppression versus p_T at high collision energy due to the partonic energy loss when jets pass through the hot dense quark-gluon matter. On the one hand, in the low p_T region, radial flow plays a major role in central collisions, which pushes protons to higher p_T regions and results in the smaller R_{cp} at low p_T . On the other hand, in the high p_T region, the Cronin effect due to the multiple nucleon-nucleon scattering effect [44,45] tends to transform the longitudinal momentum into the transverse momentum, and the effect becomes stronger with the increase in p_T in central HICs, which leads to larger R_{cp} at high p_T . For the pion case, however, its R_{cp} shows very different behavior because pions

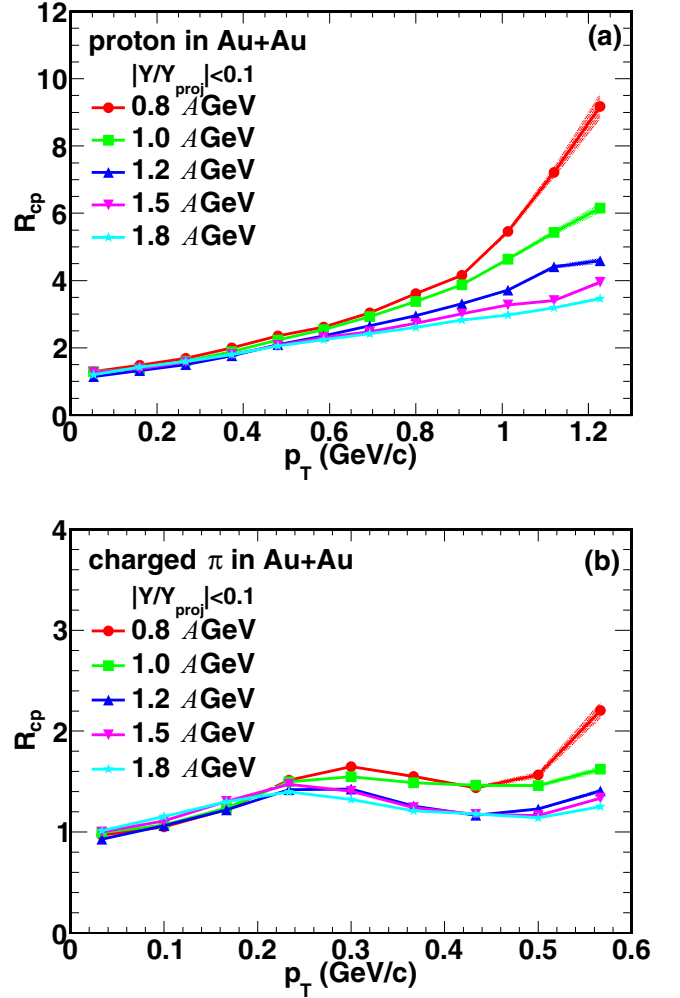


FIG. 2. R_{cp} of (a) protons and (b) pions vs p_T at different beam energies. In the calculations, $\pi N \rightarrow \Delta$ and $N\Delta \rightarrow NN$ are taken into account and the in-medium correction for NNCS is not used [i.e., $\eta = 0$ in Eq. (8)].

are produced via hard Δ decay and absorbed by nucleons with a high probability (81% in Au+Au at 1A GeV) [46]. These differences indicate the different nuclear medium effects for protons and pions.

B. Radial flow

Two important physical quantities, nuclear stopping and the radial flow, which are sensitive to the properties of nuclear bulk matter, have been extensively investigated in a wide range of incident energies from tens of MeV/nucleon to hundreds of GeV/nucleon in many experimental and theoretical works [22,47–49]. In the compression stage during a nucleus-nucleus collision, a highly dense and thermal nuclear matter medium is formed by frequent nucleon-nucleon interactions. Around 1A GeV incident energy in central heavy ion collisions, the colliding nuclei are expected to be stopped and lead to densities of $2 \sim 3$ times ρ_0 (where ρ_0 is the normal nuclear density) at the largest compression time. The nuclear stopping can be described with a ratio of transverse to parallel

quantities (e.g., energy or momentum); it reflects how much energy of the initial longitudinal motion is transferred into the internal degrees of freedom. And then, the expansion stage occurs owing to the high pressure in the compressed region. While the particles on the surface of the coupling matter zone emit outward, the inner particles frequently collide with each other, causing the probability of the outward motion to be larger than that of the inward motion, and then, the collective radial motion grows until the nuclear system freezes out. At high incident energy, hydrodynamics is suitable to describe these characteristics. A pioneering theoretical model named the blast-wave model has been put forward by Siemens and Rasmussen [50], and lots of work based on it has been carried out [19,23,51,52].

The transverse velocity distribution β_r in the region of $0 \sim R_{\max}$ is described by a self-similar profile, which is parametrized by the surface velocity β_s : $\beta_r(r) = \beta_s (\frac{r}{R})^\alpha$, where R_{\max} is the freeze-out radius, defined as the maximum radius of the expanding source at thermal freeze-out time, and the β_s is the particle radial velocity at the maximum surface where the radius is equal to the freeze-out radius, and the exponent α represents the radial flow profile, which describes the evolution of the flow velocity with the radius (if $\alpha = 0$, it means the uniform velocity; if $\alpha = 1$, it is similar to Hubble's law; and if $\alpha = 2$, it is hydrodynamical evolution).

Particle spectra are a superposition of individual thermal sources with different r , each boosting with the boost angle $\rho = \tanh^{-1} \beta_r(r)$ [19,53],

$$\frac{dn}{p_T dp_T} \propto \int_0^{R_{\max}} r dr m_T I_0 \left(\frac{p_T \sinh \rho}{T_f} \right) K_1 \left(\frac{m_T \cosh \rho}{T_f} \right), \quad (7)$$

where K_1, I_0 are the modified Bessel functions and T_f is the freeze-out temperature. The shapes of the spectra are essentially determined by the freeze-out temperature, the velocity of the transverse expansion, the flow profile, and the mass of the particle. The average flow velocity is estimated by taking an average over the transverse geometry: $\langle \beta_r \rangle = \beta_s \frac{2}{2+\alpha}$.

Figure 3(a) shows the blast-wave fitting to the p_T spectra of the Au+Au central collisions at different incident energies, namely, 0.8A, 1.0A, 1.2A, 1.5A, and 1.8A GeV. And Fig. 3(b) gives the corresponding fit parameters. From the figure, one can see that both the radial flow β and the freeze-out temperature T increase with beam energy.

V. IN-MEDIUM EFFECT

Usually the free-space nucleon-nucleon cross section $\sigma_{NN}^{\text{free}}$ obtained by experimental measurement is used as a default nucleon-nucleon cross section in the QMD model. However, the real in-medium NNCS ($\sigma_{NN}^{\text{in-medium}}$) is different from the free-space NNCS because of the effects of Pauli blocking and finite system of nuclei in heavy ion reactions, etc. In-medium two-body cross sections are therefore an indispensable component to compensate for the nuclear equation of state in the QMD simulation [7,8,10]. The in-medium NNCS can be parametrized from Particle Data Group data with medium modification which can be implemented according to the

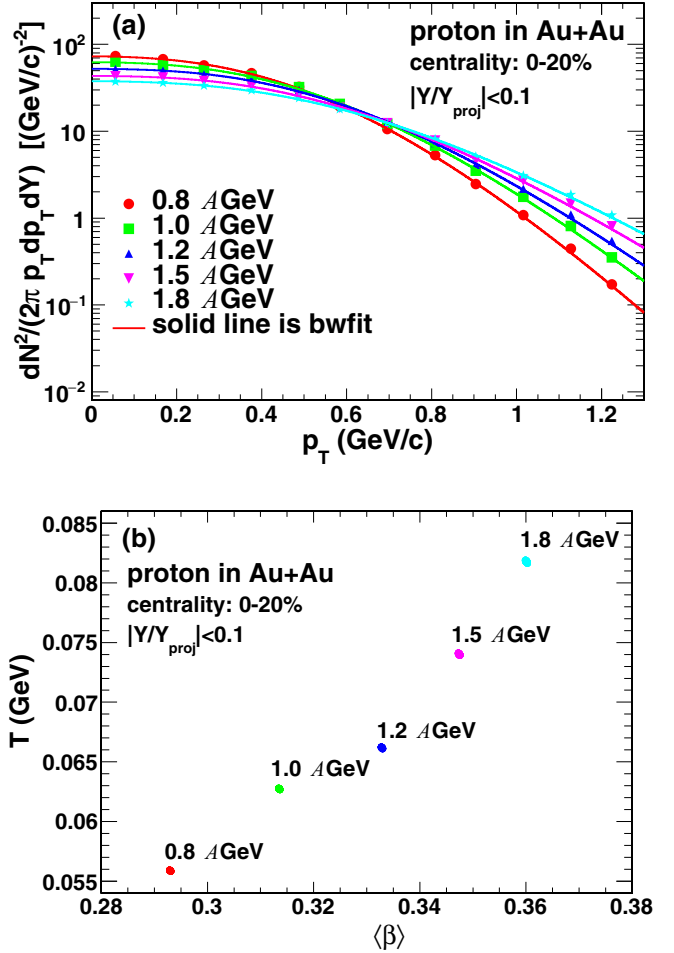


FIG. 3. Blast-wave fits to the spectra and their parameters. (a) p_T spectra in Au+Au central collisions at 0.8A, 1.0A, 1.2A, 1.5A, and 1.8A GeV, the solid lines are the blast-wave fits; (b) the blast-wave fitting contours for temperature vs radial flow at different beam energies. In the calculations, $\pi N \rightarrow \Delta$ and $N\Delta \rightarrow NN$ are taken into account and the in-medium correction for NNCS is not used [i.e., $\eta = 0$ in Eq. (8)].

density-dependent prescription [54–56]:

$$\sigma_{NN} = \sigma_{NN}^{\text{free}} \left(1 - \eta \frac{\rho}{\rho_0} \right), \quad (8)$$

where η is the in-medium NNCS reduction factor, varied between 0 and 1, ρ_0 is the normal nuclear matter density, and ρ is the local density. From this expression, the relationship between η and the in-medium effect is connected as follows:

$$\eta \uparrow \Rightarrow \sigma_{NN} \downarrow \Rightarrow \text{in-medium effect} \uparrow. \quad (9)$$

Otherwise, the in-medium NNCS scaled by the effective mass m^* , $\sigma_{NN} = \sigma_{NN}^{\text{free}} (m^*/m)^2$, has also been employed in the BUU simulation [57,58]. The latter scaling presumes that for given relative momentum, the matrix elements of interaction are not changed between the free space and medium.

In this section, the aim is to draw a conclusion on the in-medium effect by investigating on R_{cp} in different η value cases. The η values at 0.2, 0.5, and 0.9 were used in the simulation of Au+Au at 1A GeV collisions. In a previous

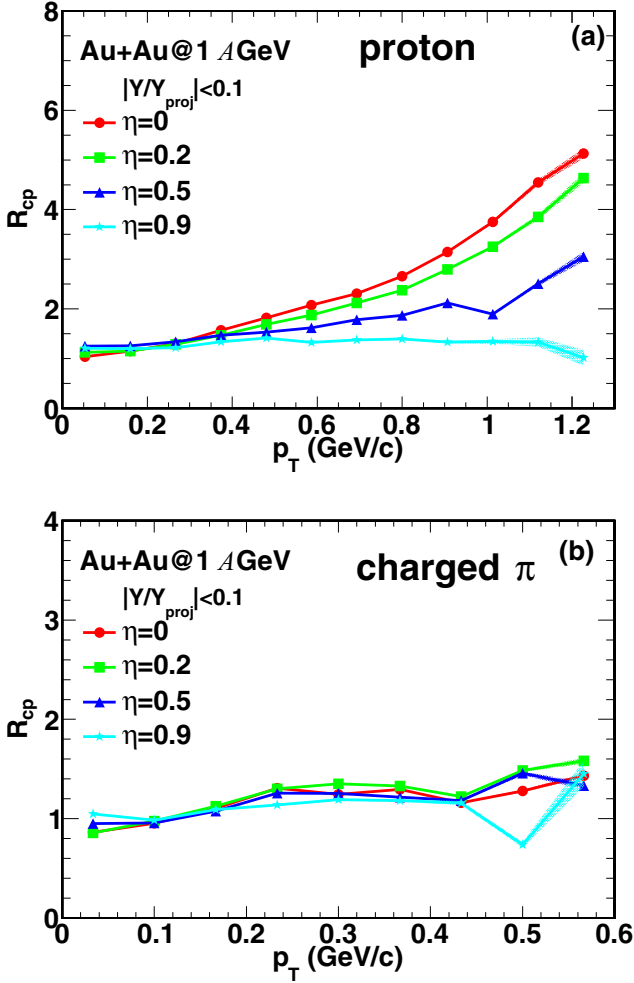


FIG. 4. Effects of the reduction factor η of the in-medium NNCS on R_{cp} of (a) protons and (b) pions. Four cases of the in-medium NNCS are considered: $\eta = 0$, $\eta = 0.2$, $\eta = 0.5$, and $\eta = 0.9$. In the calculations, $\pi N \rightarrow \Delta$ and $N\Delta \rightarrow NN$ are taken into account.

work, the value $\eta = 0.2$, i.e., 80% of the free space nucleon-nucleon cross section was obtained [59]. In fact, the medium effect is different in various ranges of incident energy and matter density [8].

A. Effect on R_{cp}

R_{cp} is a good quantity for studying the effect of the in-medium NNCS. In Fig. 4, the R_{cp} of protons and pions are shown with different η values. Due to the limited statistics, there exists fluctuation in high p_T region. The R_{cp} of protons has an increasing trend with p_T which is explained by the Cronin effect as well as radial flow [19], and its trend becomes more rapid with p_T in the low η value case because of the high collision rate between nucleons. Collisions become certainly less in higher η values and it makes the Cronin effect less significant. On the other hand, the trend of the pion R_{cp} does not seem to have any obvious change with different η value. The reason might be that the cross section for pion interaction has no significant change while the η value changes. In the next section, pion absorption will be discussed in detail.

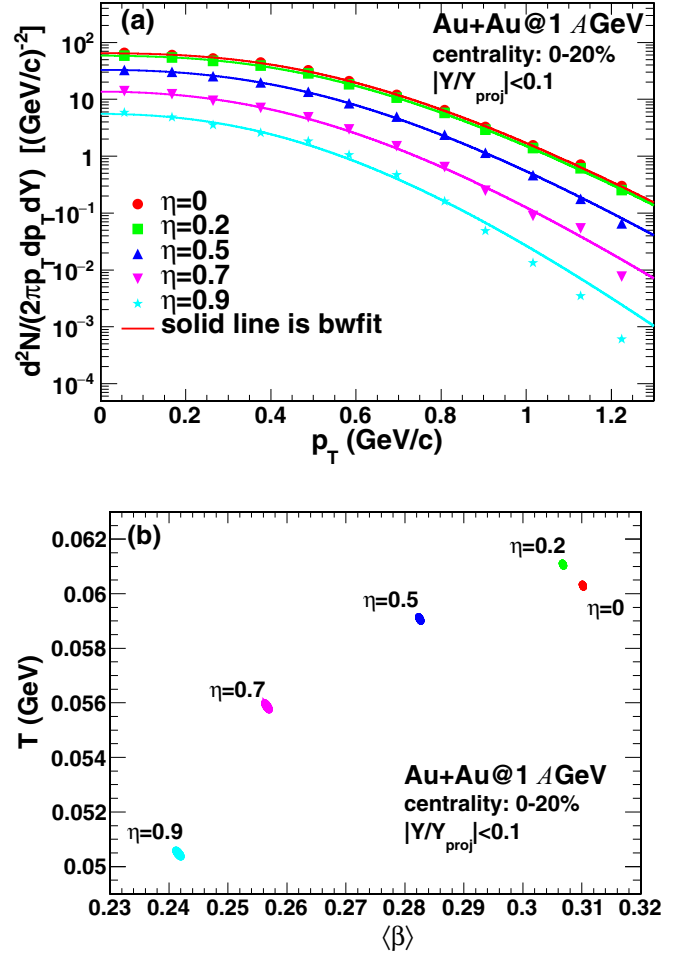


FIG. 5. Blast-wave fitting to (a) p_T spectra of protons and (b) their fitting parameters of β and T with different in-medium NNCS reduction factors in the centrality of 0–20%. In the calculations, $\pi N \rightarrow \Delta$ and $N\Delta \rightarrow NN$ are taken into account.

B. Effect on radial flow

Bauer *et al.* pointed out that in intermediate-energy HICs, nuclear stopping power is determined by both the mean field (EOS) and the in-medium nucleon-nucleon cross collisions [60]. The nuclear stopping was also proposed as a probe to extract information on the isospin dependence of the in-medium NN cross section in HICs for the beam energy starting from the Fermi energy to about 150A MeV [9]. A similar physical quantity, radial flow, is studied in this work. Figure 5(a) shows the p_T spectra from Au+Au central collisions at 1A GeV with different values of the in-medium NNCS reduction factor η (0, 0.2, 0.5, 0.7, and 0.9), fitting well with a function from the blast-wave model. In Fig. 5(b), results demonstrate that the system has smaller radial flow and lower temperature when a larger η value is taken in the simulation, i.e., smaller in-medium NNCS makes the system not too hot and leads to smaller radial flow. In contrast, a larger NNCS (i.e., smaller η value) leads to a higher temperature and larger radial flow. This picture definitely tells us the in-medium nucleon-nucleon cross section can strongly affect the system's thermal and collective behaviors.

VI. π DYNAMICS

As described in Sec. II, all pions are produced by resonance (Δ) decay in the present IQMD model since the direct pion production is very small in the intermediate-energy range and can be neglected. However, the pion absorption process has a large probability, it will obviously change the phase-space distribution of pions and even for protons. As discussed in Refs. [61,62], the pion scattering process influences the angular distribution of pions and the pion absorption channel plays an important role for the absolute number of produced pions.

We have studied the pion dynamics by modifying one or the other of the π -related channel. Because the soft Δ cannot be distinguished from all Δ including hard Δ in the present IQMD model, it is therefore not completely distinguishable between pure π absorption process and pure scattering process. Three versions of the IQMD model have been used in heavy ion collision simulation (Au+Au at 1A GeV). In the original version, both the $\pi N \rightarrow \Delta$ and the $N\Delta \rightarrow NN$ channel are retained. In the version of the deactivated soft- Δ absorption channel (without $N\Delta \rightarrow NN$ and with $\pi N \rightarrow \Delta$), the pion absorption process is suppressed and the pion scattering process is allowed. In the version of the deactivated soft- Δ production channel (without $\pi N \rightarrow \Delta$ and with $N\Delta \rightarrow NN$), both the pion absorption process and the pion scattering process are forbidden.

In Fig. 6, the azimuthal angle distributions of π^0 in the three cases are shown: the “original” case, the “no $\pi N \rightarrow \Delta$ ” case, and the “no $N\Delta \rightarrow NN$ ” case, for the centralities 0–20%, 20–40%, and 40–80%. From this figure, we can see that the pion multiplicities are obviously increasing in the no $N\Delta \rightarrow NN$ case and the no $\pi N \rightarrow \Delta$ case. An isotropic azimuthal angle distribution of π^0 appears in the no $\pi N \rightarrow \Delta$ case, while

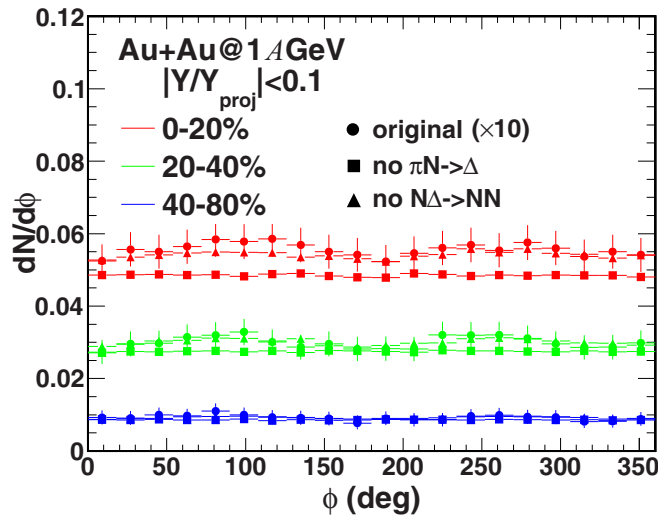


FIG. 6. Azimuthal angle distribution of π^0 in “original” case, “no $\pi N \rightarrow \Delta$ ” case, and “no $N\Delta \rightarrow NN$ ” case and different centralities (0–20%, 20–40%, and 40–80%). In the calculations, the in-medium correction for NNCS is not used [i.e., $\eta = 0$ in Eq. (8)]. In the symbols key, “original” means that both the $\pi N \rightarrow \Delta$ and $N\Delta \rightarrow NN$ are taken into account; “no $\pi N \rightarrow \Delta$ ” means that the $\pi N \rightarrow \Delta$ is turned off, but the $N\Delta \rightarrow NN$ is on; “no $N\Delta \rightarrow NN$ ” means that the $\pi N \rightarrow \Delta$ is on and the $N\Delta \rightarrow NN$ is off.

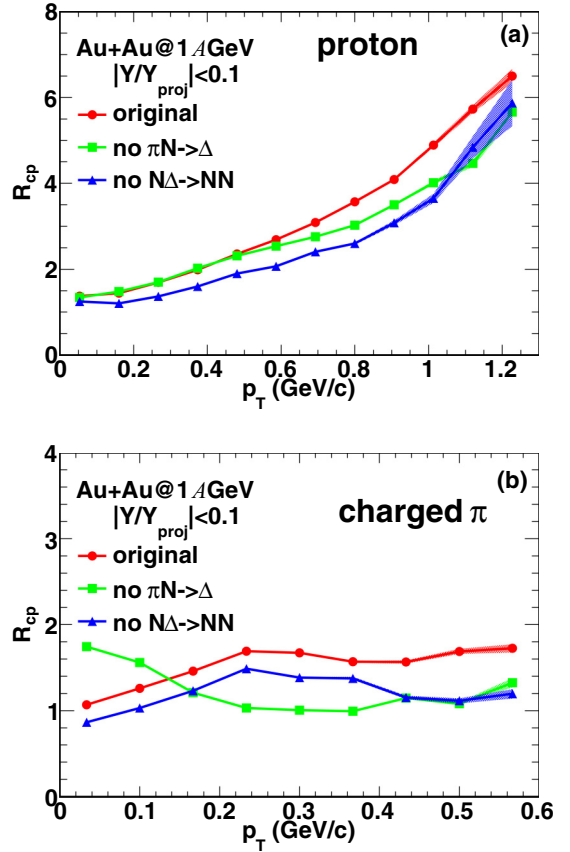


FIG. 7. R_{cp} of (a) protons and (b) pions vs p_T in Au+Au at 1A GeV by the IQMD simulation with soft EOS and MDI for the three cases. In the calculations, the in-medium correction for NNCS is not used [i.e., $\eta = 0$ in Eq. (8)].

two peaks at 90° and 270° in azimuthal angle emerge owing to the “squeezing out” effect in the original case and the no $N\Delta \rightarrow NN$ case. These results demonstrate that the pion absorption process changes the pion multiplicity, and the pion scattering process changes the π phase-space distribution.

R_{cp} of proton and pion investigated in the same three cases (original, no $\pi N \rightarrow \Delta$, and no $N\Delta \rightarrow NN$) are shown in Fig. 7. From Fig. 7(a), R_{cp} of proton in these three cases are increasing with transverse momentum, the latter two cases have lower slopes, indicating that the collision system is cold in the latter two cases. In addition, R_{cp} of charged pion in these three cases are shown in Fig. 7(b). While the R_{cp} is shifted down in the no $N\Delta \rightarrow NN$ case, the R_{cp} has an inverse trend in the no $\pi N \rightarrow \Delta$ case compared with the one in the original case. These results indicate that the pion scattering process has a major impact on pion dynamics while the pion absorption process has an important effect on π multiplicity.

VII. SUMMARY

To summarize, nuclear modification factors R_{cp} of protons and pions of Au+Au collisions from 0.8A to 1.8A GeV have been investigated by the IQMD model with the soft momentum-dependent equation of state. The R_{cp} of protons rise rapidly with the p_T increasing at 0.8A GeV owing to

radial flow and the Cronin effect. And the rising trend becomes slower as the incident energy increases. This feature can be explained by nuclear stopping whose degree decreases as the incident energy increases. On the other hand, the R_{cp} of pions rise slowly at low p_T (<0.3 GeV) and level off at high p_T (>0.3 GeV). It can be understood by these pions are produced from two sources, the hard Δ decayed pions which emit outward directly and the soft Δ decayed pions which are absorbed and then secondarily decayed. The R_{cp} of pions have a little enhancement at low p_T because these low-energy pions are affected by nucleon dynamics, such as radial flow, and they maintain a saturated trend at high p_T owing to no Cronin effect on high-energy pions.

We change the in-medium NNCS by altering the η value (0.2–0.9). Results demonstrate that radial flow in central collisions decreases when the in-medium NNCS becomes smaller (larger η value). The increasing slope of the proton R_{cp} becomes smaller with a lower in-medium NNCS, while the trend of the pion R_{cp} is changed little.

The R_{cp} of protons and pions were investigated in three cases: “original” case, “no $\pi N \rightarrow \Delta$ ” case, and “no $N\Delta \rightarrow$

NN ” case. The R_{cp} of protons have different slopes in these three cases. The R_{cp} of pions in “no $\pi N \rightarrow \Delta$ ” have an inverse trend compared with the “original” case, while the trend of R_{cp} of pions in “no $N\Delta \rightarrow NN$ ” is shifted down. This phenomenon reflects that the pion scattering process plays a dominate role in pion dynamics and the pion absorption process has significant influence on pion multiplicity, which is also supported by the azimuthal distribution of π^0 spectra.

In light of this study, we argue that the observable R_{cp} is a suitable tool to better distinguish in-medium effects of protons and pions.

ACKNOWLEDGMENTS

This work was supported in part by the Major State Basic Research Development Program in China under Contracts No. 2014CB845401 and No. 2013CB834405, the National Natural Science Foundation of China under Contracts No. 11421505, No. 11220101005, No. 11322547, No. 11275250, and No. 11205230, and the Strategic Priority Research Program of the Chinese Academy of Sciences (Grant No. XDB16).

-
- [1] J. Aichelin, *Phys. Rep.* **202**, 233 (1991).
 [2] P. Danielewicz, R. Lacey, and W. G. Lynch, *Science* **298**, 1592 (2002).
 [3] C. Hartnack, Rajeev K. Puri *et al.*, *Eur. Phys. J. A* **1**, 151 (1998).
 [4] G. F. Bertsch and S. Das Gupta, *Phys. Rep.* **160**, 189 (1988).
 [5] W. Cassing, V. Metag, U. Mosel, and K. Niita, *Phys. Rep.* **188**, 363 (1990).
 [6] B. ter Haar and R. Malfliet, *Phys. Rev. C* **36**, 1611 (1987).
 [7] G. Q. Li and R. Machleidt, *Phys. Rev. C* **48**, 1702 (1993).
 [8] X. Z. Cai, J. Feng, W. Q. Shen, Y. G. Ma, J. S. Wang, and W. Ye, *Phys. Rev. C* **58**, 572 (1998).
 [9] J.-Y. Liu, W.-J. Guo, S.-J. Wang *et al.*, *Phys. Rev. Lett.* **86**, 975 (2001).
 [10] Y. X. Zhang, Z. X. Li, and P. Danielewicz, *Phys. Rev. C* **75**, 034615 (2007).
 [11] B. Chen, F. Sammarruca, and C. A. Bertulani, *Phys. Rev. C* **87**, 054616 (2013).
 [12] I. Arsene *et al.*, *Phys. Lett. B* **650**, 219 (2007).
 [13] B. Abelev *et al.* (ALICE Collaboration), *Phys. Rev. Lett.* **110**, 082302 (2013).
 [14] K. Adcox *et al.* (PHENIX Collaboration), *Phys. Rev. Lett.* **88**, 022301 (2001).
 [15] S. S. Adler *et al.* (PHENIX Collaboration), *Phys. Rev. Lett.* **91**, 172301 (2003).
 [16] J. Adams *et al.* (STAR Collaboration), *Phys. Rev. Lett.* **91**, 172302 (2003).
 [17] B. I. Abelev *et al.* (STAR Collaboration), *Phys. Rev. Lett.* **99**, 112301 (2007).
 [18] B. I. Abelev *et al.* (STAR Collaboration), *Phys. Rev. C* **79**, 064903 (2009).
 [19] M. Lv, Y. G. Ma, G. Q. Zhang, J. H. Chen, and D. Q. Fang, *Phys. Lett. B* **733**, 105 (2014).
 [20] C. S. Zhou, Y. G. Ma, and S. Zhang, *Eur. Phys. J. A* **52**, 354 (2016).
 [21] A. Andronic, J. Lukasik, W. Reisdorf, and W. Trautmann, *Eur. Phys. J. A* **30**, 31 (2006).
 [22] G. Q. Zhang, Y. G. Ma, X. G. Cao *et al.*, *Phys. Rev. C* **84**, 034612 (2011).
 [23] W. Reisdorf *et al.* (FOPI Collaboration), *Nucl. Phys. A* **848**, 366 (2010).
 [24] C. Müntz *et al.*, *Z. Phys. A* **352**, 175 (1995).
 [25] C. L. Zhou, Y. G. Ma, D. Q. Fang, and G. Q. Zhang, *Phys. Rev. C* **88**, 024604 (2013).
 [26] J. Xu, *Nucl. Sci. Tech.* **24**, 050514 (2013).
 [27] C. L. Zhou, Y. G. Ma, D. Q. Fang, G. Q. Zhang, and X. G. Cao, *Nucl. Tech. (in Chinese)* **37**, 100516 (2014).
 [28] J. Aichelin, A. Rosenhauer, G. Peilert, H. Stoecker, and W. Greiner, *Phys. Rev. Lett.* **58**, 1926 (1987).
 [29] C. Hartnack *et al.*, *Nucl. Phys. A* **495**, 303 (1989).
 [30] C. Hartnack, H. Oeschler, Y. Leifels, E. L. Bratkovskaya, and J. Aichelin, *Phys. Rep.* **510**, 119 (2012).
 [31] S. Kumar and Y. G. Ma, *Phys. Rev. C* **86**, 051601(R) (2012).
 [32] S. Kumar and Y. G. Ma, *Nucl. Sci. Tech.* **24**, 050509 (2013).
 [33] J. Wang *et al.*, *Nucl. Sci. Tech.* **24**, 030501 (2013).
 [34] C. Tao *et al.*, *Nucl. Sci. Tech.* **24**, 030502 (2013).
 [35] Y. Zhang, Z. Li, K. Zhao, H. Liu, and M. B. Tsang, *Nucl. Sci. Tech.* **24**, 050503 (2013).
 [36] Z. Q. Feng, *Nucl. Sci. Tech.* **26**, S20512 (2015).
 [37] J. Chen, Z. Q. Feng, and J. S. Wang, *Nucl. Sci. Tech.* **27**, 73 (2016).
 [38] A. Engel, W. Cassing, U. Mosel, M. Schafer, and Gy. Wolf, *Nucl. Phys. A* **572**, 657 (1994).
 [39] S. Huber and J. Aichelin, *Nucl. Phys. A* **573**, 587 (1994).
 [40] S. Teis, W. Cassing, M. Effenberger, A. Hombach, U. Mosel, and Gy. Wolf, *Z. Phys. A* **356**, 421 (1997).

- [41] D. Pelte *et al.* (FOPI Collaboration), *Z. Phys. A* **357**, 215 (1997).
- [42] F. Antinori *et al.* (NA57 Collaboration), *Phys. Lett. B* **623**, 17 (2005).
- [43] E. Sangaline, *Nucl. Phys. A* **904-905**, 771c (2013).
- [44] D. Antreasyan, J. W. Cronin, H. J. Frisch, M. J. Shochet, L. Kluberg, P. A. Piroue, and R. L. Sumner, *Phys. Rev. D* **19**, 764 (1979).
- [45] A. H. Rezaeian and Zhun Lu, *Nucl. Phys. A* **826**, 198 (2009).
- [46] S. A. Bass, C. Hartnack, H. Stocker, and W. Greiner, *Phys. Rev. C* **51**, 3343 (1995).
- [47] F. Fu *et al.*, *Phys. Lett. B* **666**, 359 (2008).
- [48] M. A. Lisa *et al.*, *Phys. Rev. Lett.* **75**, 2662 (1995).
- [49] N. Herrmann, J. P. Wessels, and T. Wienold, *Annu. Rev. Nucl. Part. Sci.* **49**, 581 (1999).
- [50] P. J. Siemens and J. O. Rasmussen, *Phys. Rev. Lett.* **42**, 880 (1979).
- [51] B. Hong *et al.* (FOPI collaboration), *Phys. Rev. C* **58**, 603 (1998).
- [52] M. Lyv, Y. G. Ma, G. Q. Zhang *et al.*, *Nucl. Tech. (in Chinese)* **37**, 100517 (2014).
- [53] E. Schnedermann, J. Sollfrank, and U. Heinz, *Phys. Rev. C* **48**, 2462 (1993).
- [54] F. Daffin, K. Haglin, and W. Bauer, *Phys. Rev. C* **54**, 1375 (1996).
- [55] V. Prassa, G. Ferini, T. Gaitanos, H. H. Wolter, G. A. Lalazissis, and M. Di Toro, *Nucl. Phys. A* **789**, 311 (2007).
- [56] A. B. Larionov *et al.*, *Nucl. Phys. A* **696**, 747 (2001).
- [57] B. A. Li and L. W. Chen, *Phys. Rev. C* **72**, 064611 (2005).
- [58] B. A. Li, B. J. Cai, L. W. Chen, and X. H. Li, *Nucl. Sci. Tech.* **27**, 141 (2016).
- [59] D. Klakow, G. Welke, and W. Bauer, *Phys. Rev. C* **48**, 1982 (1993).
- [60] W. Bauer, *Phys. Rev. Lett.* **61**, 2534 (1988).
- [61] B. A. Li, *Nucl. Phys. A* **570**, 797 (1994).
- [62] S. A. Bass, R. Mattiello, H. Stocker, and W. Greiner, *Phys. Lett. B* **302**, 381 (1993).